# Tri-μ-bromo-bis[tribromoruthenate(III)] Salts: A Synthetic, Structural, Spectroscopic, and Electrochemical Study *

**Denise Appleby, Peter B. Hitchcock, Kenneth R. Seddon, Janet E. Turp, and Jalal A. Zora**
*School of Chemistry and Molecular Sciences, University of Sussex, Falmer, Brighton BN1 9QJ*
**Charles L. Hussey and John R. Sanders**
*Department of Chemistry, University of Mississippi, University, MS 38677, U.S.A.*
**T. Anthony Ryan**
*I.C.I. Chemicals and Polymers Group, P.O. Box 8, The Heath, Runcorn, Cheshire, WA7 4QD*

The salts $A_3[Ru_2Br_9]$ [A = Rb, Cs, or 1-ethyl-3-methylimidazolium (emim)] have been prepared, and studied by electronic absorption spectroscopy and electrochemistry in both conventional solvents and a basic room-temperature ionic liquid, $AlBr_3$–[emim]Br: the mixed-valence complex $[Ru_2Br_9]^{4-}$ was generated on the electrochemical time-scale in the latter medium. The caesium and rubidium salts were characterized by powder *X*-ray diffraction, and the structure of the $[emim]^+$ salt was determined by single-crystal *X*-ray diffraction: the anion is an almost idealized confacial bioctahedron, but there is a significant metal–metal interaction [*r*(RuRu) = 0.288 0(3) nm]. Literature reports that $A_4[Ru_2OBr_{10}]$ (A = Rb or Cs) had been prepared and characterized are shown to be erroneous: the products are mixtures of $A_3[Ru_2Br_9]$ and ABr.

There have been a number of reports of the preparation of salts of the μ-oxo-bis[pentabromoruthenate(IV)] anion, $[Ru_2OBr_{10}]^{4-}$.[1a] Unfortunately, the majority of these reports have relied more upon arguments based upon analogy with the well characterized chloride complexes, $[Ru_2OCl_{10}]^{4-}$,[2,3] than upon hard structural or spectroscopic data. The only significant claim is that of San Filippo *et al.*,[4,5] who have reported a detailed synthetic procedure for $Cs_4[Ru_2OBr_{10}]$, as well as describing its electronic absorption, Raman, and resonance-Raman spectra. In a preliminary communication,[6] we demonstrated that the purported $Cs_4[Ru_2OBr_{10}]$ was in fact a 1:1 mixture of caesium bromide and the recently reported $Cs_3[Ru_2Br_9]$.[7] Here we give full particulars of that work, along with details of the crystal structure of $[emim]_3[Ru_2Br_9]$ (emim = 1-ethyl-3-methylimidazolium), and its electrochemical and spectroscopic properties in a novel basic $AlBr_3$–[emim]Br ionic liquid.[8] In particular, we have drawn on the seminal work of Stephenson and co-workers,[9] for comparison of the spectral and electrochemical properties of tri-μ-bromo-bis[tribromoruthenate(III)] salts in ionic liquids with those in conventional organic solvents.

## Experimental

*General Techniques.*—Electronic absorption spectra were recorded with a Varian Cary 2300 spectrophotometer using either 1- or 0.1-cm cells. Baselines were recorded at 0.2 nm $s^{-1}$, and spectral data were collected at 1 nm $s^{-1}$. Infrared spectra (Nujol mulls, CsI windows) were recorded with a Perkin-Elmer PE177 spectrophotometer (4 000—200 $cm^{-1}$), and calibrated with reference to indene (381 $cm^{-1}$). Microanalytical data were determined by the microanalytical service of the University of Sussex.

Powder *X*-ray diffraction data were obtained using a Guinier camera (I.C.I., Runcorn). The Cu-$K_\alpha$ radiation (λ = 0.154 1834 nm) was produced by a Philips 1130 generator operating at 50 kV and 50 mA, using a graphite monochromator and scintillation counter. The samples were finely ground, placed in a standard deep-pack Philips rotating specimen holder, and scanned over a 2θ range of 4—70° on a 2-s count with 50 points per degree. The data were collected by a PDP-11/35 computer, and processed on a DEC 10. The precision of a data point determination is ±0.025°. The system was calibrated with KBr, RbBr, and CsBr, and a scaling factor of 0.9974 was applied to all determined $a_0$ and $c_0$ values.

Electrochemical experiments in the $AlBr_3$–[emim]Br ionic liquid were carried out inside a glove-box filled with dry, dioxygen-free dinitrogen. The glove-box system, electrochemical cell, glassy carbon working electrode, and thermostatted furnace used have been described.[10,11] Electrochemical experiments were conducted with an AMEL model 551 potentiostat coupled to a PARC model 175 universal programmer. Data were recorded on either a Houston Instruments model 100 X-Y/Y-t recorder or a Nicolet Explorer I digital oscilloscope. All potentials are reported *versus* an aluminium electrode immersed in the 66.7:33.3 mol % $AlBr_3$–[emim]Br melt. The reference electrode compartment was separated from the bulk melt with a fine-porosity frit.

Reagents were purchased from either Aldrich or B. D. H., and used as received unless otherwise stated. Aluminium(III) bromide (ex Fluka) was multiply sublimed from aluminium metal (ex Goodfellows) and sodium bromide prior to use, and 1-methylimidazole was purified by distillation. The ionic liquids were prepared by the literature procedure.[8] Hydrobromic acid (6 mol $dm^{-3}$) was purified by distillation immediately prior to use. Commercial hydrated 'ruthenium(III) chloride' (ex Johnson Matthey)[1b] was used as received.

*Preparation of 1-Ethyl-3-methylimidazolium Bromide.*—Bromoethane (50 $cm^3$, 0.45 mol) and 1-methylimidazole (10 $cm^3$, 0.18 mol) were heated under dry dinitrogen at reflux for 48 h, whence a white-yellow mass formed. This solid was collected by filtration, and recrystallized twice from ethanenitrile (30 $cm^3$) and ethyl ethanoate (10 $cm^3$). The white anhydrous crystals were then dried *in vacuo* and stored under dinitrogen.

*Preparation of Ruthenium(IV) Oxide.*—Commercial hydrated 'ruthenium(III) chloride' (2 g, 7.95 mmol) was dissolved in hydrochloric acid (20 $cm^3$, 4 mol $dm^{-3}$) to give a dark brown

* *Supplementary data available:* see Instructions for Authors, *J. Chem. Soc., Dalton Trans.*, 1990, Issue 1, pp. xix—xxii.

solution. Concentrated aqueous sodium hydroxide solution (*ca.* 10 $cm^3$) was then slowly added; at the neutralization point, a thick dense black precipitate formed. This solid was collected by filtration, and then washed copiously with water (*ca.* 3 l), until the washings were free of chloride ions [test: acidic aqueous silver(I) nitrate solution]. The solid was then dried *in vacuo* over silica gel for 2 d to yield a black powder.

*Preparation of Hydrated 'Ruthenium*(III) *Bromide'*.[1c]—Ruthenium(IV) oxide (2 g, 15 mmol) was added to an excess of hydrobromic acid (100 $cm^3$, 6 mol $dm^{-3}$): the reaction was slightly exothermic, and an initial greenish tint was replaced within a few seconds by an orange-brown colour. The mixture was then heated in air until the majority of the hydrobromic acid had evaporated to yield a thick resinous red residue, which was cooled and dried *in vacuo* for 2 d [N.B. heating the mixture to dryness should be avoided, as irreversible decomposition to ruthenium(IV) oxide occurs].

*Preparation of Ruthenium*(VIII) *Oxide*.—Ruthenium(IV) oxide (1 g, 7.52 mmol) and sodium iodate(VII) (5 g, 23.3 mmol) were added to water (30 $cm^3$, 0 °C) and stirred at 0 °C until all of the ruthenium(IV) oxide had reacted and a bright yellow solution had formed. In a sealed flow system, dinitrogen was passed through this solution to carry the volatile product into an ice-cold receiver, usually containing hydrobromic acid (20 $cm^3$, 3 mol $dm^{-3}$).

*Attempted Preparation of Rubidium* μ-*Oxo-bis*[*pentabromoruthenate*(IV)] *by a Method based on that of San Filippo* et al.[4,5]—An orange-brown solution of ruthenium(VIII) oxide in hydrobromic acid (20 $cm^3$, 3 mol $dm^{-3}$; see above) was placed in a stoppered flask and stirred for 24 h. Its volume was then reduced by half under reduced pressure, and a solution of rubidium bromide (2.75 g, 1.66 mmol) in hydrobromic acid (15 $cm^3$, 6 mol $dm^{-3}$) was added. The resulting red solution was boiled in air for 1 min, and allowed to stand at ambient temperature for 24 h, whence a fine purple-black precipitate formed. This solid was collected by filtration, washed with ice-cold water (0.5 $cm^3$), and dried *in vacuo* for 4 d.

*Attempted Preparation of Caesium* μ-*Oxo-bis*[*pentabromoruthenate*(IV)].—The above procedure was followed, except that caesium bromide (3.5 g, 1.64 mmol) replaced rubidium bromide.

*Attempted Preparation of Rubidium* μ-*Oxo-bis*[*pentabromoruthenate*(IV)] *by a Variation of the Method of San Filippo* et al.[4,5]—A solution of rubidium bromide (3 g, 1.81 mmol) in hydrobromic acid (20 $cm^3$, 6 mol $dm^{-3}$) was added to a freshly prepared solution of ruthenium(VIII) oxide in hydrobromic acid (20 $cm^3$, 3 mol $dm^{-3}$; see above). The resultant solution was allowed to stand at ambient temperature for 12 h, whence a fine purple-black precipitate formed. This solid was collected by filtration, washed with ice-cold hydrobromic acid (2 $cm^3$, 6 mol $dm^{-3}$), and dried *in vacuo* for 2 d.

*Attempted Preparation of Caesium* μ-*Oxo-bis*[*pentabromoruthenate*(IV)].—The above procedure was followed, except that caesium bromide (3.5 g, 1.64 mmol) replaced rubidium bromide.

*By a variation of the method of Crisp*[12] *for the synthesis of* $Cs_4[Ru_2OCl_{10}]$. Hydrated 'ruthenium(III) bromide' (1.59 g, 0.43 mmol) was dissolved in water (10 $cm^3$) to form a dark red solution. Hydrogen peroxide (1 $cm^3$, 30 wt % in water) was added very slowly, in order to completely oxidize the ruthenium(III) to ruthenium(IV), and the solution was reduced in volume (to *ca.* 7 $cm^3$) at 100 °C and allowed to cool to ambient temperature. Hydrobromic acid (4 $cm^3$, 6 mol $dm^{-3}$) and caesium bromide (2.13 g, 1.00 mmol) were then added, and the solution was shaken for 1 h. The dense black precipitate that formed was collected by filtration, washed with ice-cold hydrobromic acid (2 $cm^3$, 6 mol $dm^{-3}$) and ethanol, and dried *in vacuo* for 2 d.

*Preparation of Rubidium Tri*-μ-*bromo-bis*[*tribromoruthenate*(III)].—Hydrated 'ruthenium(III) bromide' (0.5 g, 1.27 mmol) was added to hydrobromic acid (20 $cm^3$, 6 mol $dm^{-3}$) and gently heated in air (*ca.* 10 min); any undissolved residue was removed by filtration. Rubidium bromide (0.54 g, 3.27 mmol) in hydrobromic acid (20 $cm^3$, 6 mol $dm^{-3}$) was added to this warm red solution, followed by ethanol (80 $cm^3$). The purple-red solution was then vigorously heated in air until its volume was reduced to approximately half. It was then allowed to cool to room temperature and left at −25 °C for 48 h. The resulting black precipitate was collected by filtration, washed with ice–cold water (0.5 $cm^3$), and dried *in vacuo* for 2 d.

*Preparation of Caesium Tri*-μ-*bromo-bis*[*tribromoruthenate*(III)].—Hydrated 'ruthenium(III) bromide' (0.5 g, 1.27 mmol) was added to hydrobromic acid (20 $cm^3$, 6 mol $dm^{-3}$) and gently heated in air (*ca.* 10 min); any undissolved residue was removed by filtration. Caesium bromide (0.41 g, 1.93 mmol) in hydrobromic acid (20 $cm^3$, 6 mol $dm^3$) was slowly added to this warm red solution while gently shaking, whence a small amount of black solid formed. The solution was then vigorously heated in air until its volume was reduced by *ca.* one third. It was then cooled to room temperature and left at 3 °C for 12 h. The resulting purple-black precipitate was collected by filtration, washed with ice-cold water (0.5 $cm^3$), and dried *in vacuo* for 2 d.

*Preparation of* 1-*Ethyl*-3-*methylimidazolium Tri*-μ-*bromo-bis*-[*tribromoruthenate*(III)].—Hydrated 'ruthenium(III) bromide' (0.5 g, 1.27 mmol) was added to hydrobromic acid (20 $cm^3$, 6 mol $dm^{-3}$), left at ambient temperature for 2 h, and then saturated with bromine gas (carried in a stream of dinitrogen); any undissolved solid was removed by filtration at this stage. 1-Ethyl-3-methylimidazolium bromide (0.481 g, 2.53 mmol) in hydrobromic acid (3 $cm^3$, 6 mol $dm^{-3}$) was added to the orange-brown solution, which was then stored at 3 °C for 7 d. The volume of the solution was then reduced by half by heating in air, and the resultant red solution was cooled to ambient temperature. Addition of ethanol (500 $cm^3$), followed by diethyl ether (2 l), produced a purple precipitate; the mixture was then allowed to stand at 3 °C for 12 h, and the resulting needle-shaped crystals were collected by filtration and dried *in vacuo* (Found: C, 17.00; H, 2.90; N, 6.35. Calc. for $C_{18}H_{33}Br_9N_6Ru_2$: C, 17.25; H, 2.65; N, 6.70%).

*Determination of the Crystal Structure of* 1-*Ethyl*-3-*methylimidazolium Tri*-μ-*bromo-bis*[*tribromoruthenate*(III)].—Purple-black needle-like crystals were prepared as described above; a crystal of dimensions 0.22 × 0.12 × 0.1 mm was used for all crystallographic measurements, which were made with graphite-monochromated Mo-$K_\alpha$ radiation (λ = 0.071 069 nm) and an Enraf-Nonius CAD4 diffractometer.

*Crystal data*. $C_{18}H_{33}Br_9N_6Ru_2$, $M$ = 1 245.8, monoclinic, space group $P2_1/c$, $a$ = 1.922(2), $b$ = 1.084(2), $c$ = 1.896(2) nm, β = 119.7(3)°, $U$ = 3.4325 $nm^3$, $Z$ = 4, $D_c$ = 2.42 g $cm^{-3}$, $F(000)$ = 2 344, μ(Mo-$K_\alpha$) = 119.8 $cm^{-1}$.

*Data collection and processing*. The intensities of 4 845 *hkl* and *hkl̄* reflections with 2 < θ < 25° were measured by the θ—2θ scan technique; the scan width was 0.8 + 0.35 tan θ°. The integrated intensities, $I$, and their variances, σ($I$), were corrected for Lorentz, polarization, and absorption effects (using ψ-scan measurements for six reflections). Absorption correction factors

**Table 1.** Fractional atomic co-ordinates with standard deviations in parentheses for $[emim]_3[Ru_2Br_9]$ ($\times 10^4$ for Ru and Br, $\times 10^3$ for other atoms)

| Atom | x | y | z | Atom | x | y | z |
|---|---|---|---|---|---|---|---|
| Ru(1) | 2 078(2) | 2 562(4) | 5 118(2) | C(6) | 53(3) | 657(6) | 468(3) |
| Ru(2) | 3 026(2) | 350(4) | 5 477(2) | N(3) | 651(3) | 412(7) | 261(3) |
| Br(1) | 606(3) | 2 684(6) | 4 102(3) | N(4) | 752(3) | 347(5) | 270(3) |
| Br(2) | 1 867(3) | 3 811(6) | 6 100(3) | C(7) | 717(3) | 344(6) | 302(3) |
| Br(3) | 2 347(3) | 4 514(6) | 4 573(3) | C(8) | 611(6) | 434(13) | 289(7) |
| Br(4) | 3 544(3) | 2 413(5) | 6 115(3) | C(9) | 647(3) | 456(7) | 197(3) |
| Br(5) | 2 250(3) | 1 313(5) | 4 095(3) | C(10) | 707(0) | 416(0) | 207(0) |
| Br(6) | 1 835(3) | 627(5) | 5 687(3) | C(11) | 831(7) | 261(13) | 280(7) |
| Br(7) | 2 534(3) | −1 742(6) | 4 866(3) | C(12) | 825(6) | 183(11) | 224(6) |
| Br(8) | 3 797(3) | −623(6) | 6 854(3) | N(5) | 619(2) | 819(5) | 142(2) |
| Br(9) | 4 188(3) | 129(6) | 5 255(3) | N(6) | 513(2) | 798(4) | 25(2) |
| N(1) | −11(2) | 951(4) | 284(2) | C(13) | 596(3) | 818(7) | 60(3) |
| N(2) | 3(2) | 846(5) | 393(2) | C(14) | 705(3) | 827(7) | 205(3) |
| C(1) | 32(3) | 917(6) | 353(3) | C(15) | 556(4) | 818(9) | 151(5) |
| C(2) | 12(3) | 1 038(7) | 238(3) | C(16) | 491(4) | 788(8) | 65(4) |
| C(3) | −78(3) | 886(5) | 255(3) | C(17) | 459(3) | 775(6) | −64(3) |
| C(4) | −75(4) | 833(7) | 299(4) | C(18) | 403(7) | 717(14) | −68(7) |
| C(5) | 41(3) | 791(5) | 466(3) | | | | |

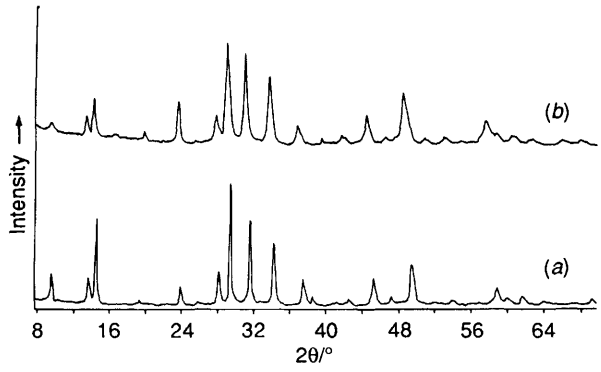


**Figure 1.** *X*-Ray powder diffraction patterns for (*a*) $Rb_3[Ru_2Br_9]$ and (*b*) $Cs_3[Ru_2Br_9]$

**Table 2.** Lattice parameters and i.r. data for $A_3[Ru_2Br_9]$

| A | $a_0$/nm | $c_0$/nm | $\nu(RuBr)_t$/cm$^{-1}$ | Ref. |
|---|---|---|---|---|
| Rb | 0.7356 | 1.7901 | 260, 240 | This work |
| Rb | 0.7344 | 1.8031 | 263, 242 | 7 |
| Cs | 0.7529 | 1.8318 | 258, 236 | This work |
| Cs | 0.7526 | 1.8363 | 259, 240 | 7 |
| emim | | | 254, 228 | This work |

were between 0.71 and 0.97. Rejection of the reflections with $I \leqslant \sigma(I)$ yielded 2 632 independent structure amplitudes that were used in all subsequent calculations.

*Structure solution and refinement.* The Ru and Br atoms were located by direct methods using MULTAN.[13] The remaining non-hydrogen atoms of the three cations (18 carbon atoms and 6 nitrogen atoms) were located from a difference map. The Ru and Br atoms were anisotropically refined, while other non-hydrogen atoms were refined isotropically. During the refinement, C(10) consistently moved away from the original peak position, giving large shifts and a high thermal parameter. It was therefore finally fixed at the position from the map. Complex neutral-atom scattering factors[14] were used throughout. Refinement converged (shift/e.s.d. < 0.62) at $R = 0.097$, $R' = 0.155$ for 436 structural parameters. These residual values are high, which is probably due to the quality of the data from the rather poor crystal combined with a high absorption coefficient. In the final difference Fourier map the highest peak was 2.0 e Å$^{-3}$. The final fractional atomic co-ordinates are shown in Table 1. All calculations were performed on a PDP-11/34 computer, using the Enraf-Nonius structure determination package.

Additional material available from the Cambridge Crystallographic Data Centre comprises thermal parameters and remaining bond lengths and angles.

## Results and Discussion

*The Preparation of Tri-μ-bromo-bis[tribromoruthenate(III)] Salts.*—The two published routes to salts of the $[Ru_2Br_9]^{3-}$ anion both involve reaction of a chlororuthenium reagent (typically, $RuCl_3 \cdot xH_2O$) with an excess of a hydrobromic acid–ethanol mixture, followed by the addition of a salt, ABr, which results in the isolation of the salt $A_3[Ru_2Br_9]$.[7,9] The procedure described here is based on that of Stephenson and co-workers,[9] differing in that the ruthenium reagent used is a bromoruthenium species [hydrated 'ruthenium(III) bromide', a heterogeneous mixture analogous to commercial hydrated 'ruthenium(III) chloride'].[1b,c] Heating this in the presence of ethanol ensures that the ruthenium present is all in oxidation state +3. This modification has the advantage that the possibility of chloride contamination of the products is significantly reduced, an important feature when preparing samples for electrochemical studies in ionic liquids. Three salts, $A_3[Ru_2Br_9]$ (A = Rb, Cs, or emim), were prepared, usually in low yields (typically 7—35%) owing to their extreme solubility in hydrobromic acid. Although many attempts were made to isolate $K_3[Ru_2Br_9]$, we were unsuccessful in preparing a sample which was totally free of potassium bromide as a minor contaminant.

*The Characterization of Tri-μ-bromo-bis[tribromoruthenate(III)] Salts.*—The *X*-ray powder diffraction patterns for $Rb_3[Ru_2Br_9]$ and $Cs_3[Ru_2Br_9]$ are illustrated in Figure 1. They are both classically hexagonal patterns,[15] and the values of $a_0$ and $c_0$ were derived by linear extrapolation of the Nelson–Riley function (see Appendix). Agreement with the literature values[7] is good (see Table 2), despite the fact that the method of parameter determination was not specified.[7] It should also be noted that the *X*-ray diffraction patterns for these $A_3[Ru_2Br_9]$ salts contain all the lines that are characteristic of $A_2[RuBr_6]$ salts,[7,16] but the relative intensities of the lines are significantly different.

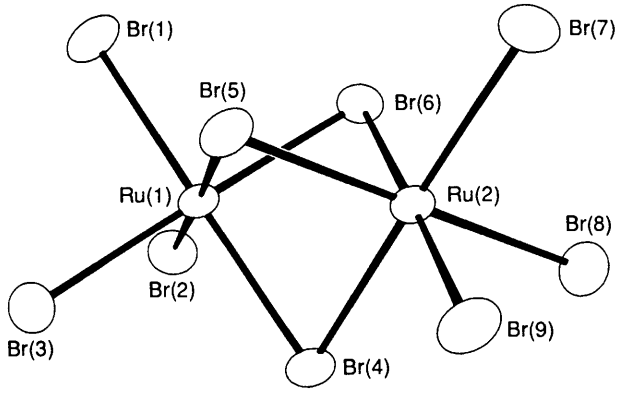


**Figure 2.** The structure of the anion in $[emim]_3[Ru_2Br_9]$

**Table 3.** Intraionic distances (nm) and bond angles (°) in the anion of $[emim]_3[Ru_2Br_9]$, with estimated standard deviations shown in parentheses

| | | | |
|---|---|---|---|
| Ru(1)–Br(1) | 0.251 7(3) | Ru(1)–Br(2) | 0.249 6(3) |
| Ru(1)–Br(3) | 0.251 8(4) | Ru(1)–Br(4) | 0.250 2(3) |
| Ru(1)–Br(5) | 0.251 8(3) | Ru(1)–Br(6) | 0.250 7(3) |
| Ru(2)–Br(4) | 0.250 3(3) | Ru(2)–Br(5) | 0.251 3(3) |
| Ru(2)–Br(6) | 0.253 0(3) | Ru(2)–Br(7) | 0.250 8(3) |
| Ru(2)–Br(8) | 0.250 9(3) | Ru(2)–Br(9) | 0.248 1(3) |
| Br(1)–Ru(1)–Br(2) | 90.3(1) | Br(1)–Ru(1)–Br(3) | 91.3(1) |
| Br(1)–Ru(1)–Br(4) | 179.1(1) | Br(1)–Ru(1)–Br(5) | 88.0(1) |
| Br(1)–Ru(1)–Br(6) | 89.7(1) | Br(2)–Ru(1)–Br(3) | 89.6(1) |
| Br(2)–Ru(1)–Br(4) | 90.5(1) | Br(2)–Ru(1)–Br(5) | 178.3(1) |
| Br(2)–Ru(1)–Br(6) | 89.9(1) | Br(3)–Ru(1)–Br(4) | 88.9(1) |
| Br(3)–Ru(1)–Br(5) | 90.2(1) | Br(3)–Ru(1)–Br(6) | 178.8(1) |
| Br(4)–Ru(1)–Br(5) | 91.1(1) | Br(4)–Ru(1)–Br(6) | 90.1(1) |
| Br(5)–Ru(1)–Br(6) | 90.4(1) | Br(4)–Ru(2)–Br(5) | 91.2(1) |
| Br(4)–Ru(2)–Br(6) | 89.5(1) | Br(4)–Ru(2)–Br(7) | 178.6(1) |
| Br(4)–Ru(2)–Br(8) | 89.1(1) | Br(4)–Ru(2)–Br(9) | 89.6(1) |
| Br(5)–Ru(2)–Br(6) | 90.0(1) | Br(5)–Ru(2)–Br(7) | 90.1(1) |
| Br(5)–Ru(2)–Br(8) | 179.7(1) | Br(5)–Ru(2)–Br(9) | 88.9(1) |
| Br(6)–Ru(2)–Br(7) | 91.0(1) | Br(6)–Ru(2)–Br(8) | 89.9(1) |
| Br(6)–Ru(2)–Br(9) | 178.6(1) | Br(7)–Ru(2)–Br(8) | 89.6(1) |
| Br(7)–Ru(2)–Br(9) | 90.0(1) | Br(8)–Ru(2)–Br(9) | 91.1(1) |
| Ru(1)–Br(4)–Ru(2) | 70.28(9) | Ru(1)–Br(5)–Ru(2) | 69.87(9) |
| Ru(1)–Br(6)–Ru(2) | 69.77(9) | | |

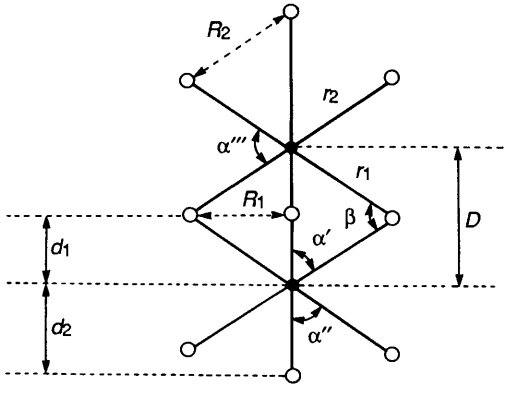


**Figure 3.** The principal structural parameters which define a general confacial bioctahedral configuration

The i.r. spectra of the salts $A_3[Ru_2Br_9]$ (A = Rb, Cs, or emim) clearly show the two strong terminal ν(RuBr) i.r.-active bands expected for the $D_{3h}$ symmetry of the confacial bioctahedral anion. The anticipated single i.r.-active band for the bridging bromides was not observed, but almost certainly lies below 200 $cm^{-1}$ [since, normally, $\nu(MBr)_b$ is approximately $0.7\nu(MBr)_t$].[17]

*The Crystal Structure of* 1-*Ethyl*-3-*methylimidazolium Tri*-μ-*bromo-bis*[*tribromoruthenate*(III)].—The unit cell of $[emim]_3[Ru_2Br_9]$ shows that there are no interionic contacts shorter than the sum of the van der Waals radii, and the closest contacts {r[Br(2)···N(4)] = 0.357, r[Br(9)···N(6)] = 0.365, r[Br(1)···N(1)] = 0.385, r[Br(1)···C(3)], r[Br(7)···N(18)] = 0.356, r[Br(9)···C(18)] = 0.373, and r[Br(3)···C(3)] = 0.357 nm} do not involve the carbon atom [C(1), C(7), or C(13)] between the two nitrogen atoms of the imidazole ring. This suggests that, unlike the structure of [emim] I,[18] which contains a strong hydrogen-bonding interaction between the anion and the cation, there is no significant hydrogen bonding present in the lattice of $[emim]_3[Ru_2Br_9]$.

The structures and geometries of the cations are poorly defined (being adversely affected by the existence of the eleven heavy atoms of the anion), but are well determined in the structures of [emim]I,[18] $[emim]_2[UO_2Cl_4]$,[19] and $[emim]_2[UCl_6]$:[19] there is nothing to indicate any remarkable features in their structure. In contrast, the structure of the anion (Figure 2) is well determined, and its dimensions are detailed in Table 3. It possesses the expected confacial bioctahedral structure, with a ruthenium–ruthenium separation of 0.2880(3) nm (*cf.* 0.286 nm, as estimated from *X*-ray powder diffraction data upon $Cs_3[Ru_2Br_9]$).[7] This anion forms one of a growing class of isostructural complexes of the general type $[M_2X_9]^{3-}$ (M = Ru, X = Cl;[20] M = Mo, X = Cl or Br;[21] M = Cr, X = Cl or Br;[21,22] M = W, X = Cl;[23] M = Rh, X = Cl;[24] M = Tl, X = Cl;[25] M = Bi, X = I;[26] M = Ti, X = Cl[27]), which contain varying degrees of metal–metal interaction. The idealized structure[24] would have the terminal and bridging bonds of equal length, all the X–M–X angles at 90°, the M–X–M angles at 70.53°, and each metal atom precisely halfway between the planes defined by its sets of terminal halide ligands and the set of bridging halide ligands. Figure 3 illustrates and defines the three principal structural parameters ($d_1/d_2$, α′, and β) that Cotton and Ucko[24] use to describe distortions from this idealized geometry. These distortions arise from elongation or compression of the structure along the metal–metal vector (the $C_3$ axis), and Table 4 compares these parameters for $[Ru_2Br_9]^{3-}$ with those for related systems. In fact, the angles (β − 70.53)° and (90 − α′)° are more convenient to use, as these give a direct indication of the distortion from ideality. It is tempting to equate the idealized structure with the absence of metal–metal bonding, but this is fallacious, as the absence of a metal–metal bond implies the existence of positive metal–metal repulsions, which would result in $d_1/d_2 > 1$, (β − 70.53) > 0, and (90 − α′) > 0. Examination of Table 4 with $[Ru_2Br_9]^{3-}$ as the cynosure reveals the following trends.

(*a*) In every case in which bromides and chlorides of the same metal have been studied, the metal–metal bond for the bromide complex is longer. Thus, for $[Ru_2Br_9]^{3-}$, the metal–metal bond is 0.0155 nm longer than for its chloride analogue; similarly, for molybdenum and chromium the equivalent parameters are 0.0161 and 0.0197 nm, respectively. This is a reflection of the larger size of the bromide ion compared with the chloride ion.

(*b*) For cases where there is no metal–metal bonding (M = Cr, Rh, Tl, Bi, or Ti), the ratio $d_1/d_2$ is between 1.20 and 1.62. Where there is unambiguous metal–metal bonding (Mo or W), this ratio is between 0.9 and 1.0. For $[Ru_2Br_9]^{3-}$, the ratio is 1.001, close to that for the molybdenum complexes, and indicative of the presence of significant metal–metal bonding.

(*c*) The parameters $d_1/d_2$, (β − 70.53), and (90 − α′), for $[Ru_2Br_9]^{3-}$, take the values 1.001, −0.557°, and −0.675°, respectively. Thus, the structure of $[Ru_2Br_9]^{3-}$ is an almost idealized confacial bioctahedron (indeed the most perfect

**Table 4.** Structural parameters * for $[M_2X_9]^{n-}$ in $A_n[M_2X_9]$

| $A^+$ = | $[Ru_2Br_9]^{3-}$ [emim]$^+$ | $[Ru_2Cl_9]^{3-}$ $Cs^+$ | $[Mo_2Br_9]^{3-}$ $Cs^+$ | $[Mo_2Cl_9]^{3-}$ $Cs^+$ | $[Cr_2Cl_9]^{3-}$ $Cs^+$ | $[Cr_2Br_9]^{3-}$ $Cs^+$ | $[W_2Cl_9]^{3-}$ $K^+$ | $[Rh_2Cl_9]^{3-}$ $[NMe_3Ph]^+$ | $[Tl_2Cl_9]^{3-}$ $Cs^+$ | $[Bi_2I_9]^{3-}$ $Cs^+$ | $[Ti_2Cl_9]^-$ $[PCl_4]^+$ |
|---|---|---|---|---|---|---|---|---|---|---|---|
| Ref. | This work | 20 | 21 | 21 | 22 | 21 | 23 | 24 | 25 | 26 | 27 |
| $D$/nm | 0.288 0(3) | 0.2725 | 0.2816 | 0.2655 | 0.3120 | 0.3317 | 0.241 | 0.3121 | 0.37 | 0.4051 | 0.3430 |
| $r_1$/nm | 0.251 2(9) | 0.2391 | 0.2624 | 0.2487 | 0.252 | 0.2577 | 0.250 | 0.2397 | 0.28 | 0.3249 | 0.2493 |
| $r_2$/nm | 0.250 8(11) | 0.2332 | 0.2544 | 0.2384 | 0.234 | 0.2417 | 0.240 | 0.2296 | 0.25 | 0.2923 | 0.2133 |
| $R_1$/nm | 0.3564 | 0.3403 | 0.3834 | 0.3643 | 0.344 | 0.3417 | 0.380 | 0.3151 | 0.37 | 0.4206 | 0.3137 |
| $R_2$/nm | 0.3551 | | 0.3620 | 0.3401 | 0.341 | 0.3527 | 0.340 | 0.3314 | 0.37 | 0.4193 | 0.3343 |
| $\alpha'$/° | 90.7 | 90.7 | 93.89 | 94.2 | 85.8 | 83.0 | 98 | 82.2 | 82 | 85.25 | 78.1 |
| $\alpha''$/° | 90.3 | 90.3 | 90.73 | 91.0 | 93.3 | 93.7 | 91 | 92.4 | 97 | 94.13 | 98.1 |
| $\alpha'''$/° | 89.8 | 89.5 | 87.65 | 87.4 | 90.1 | 91.4 | 85 | 92.5 | 90 | 90.11 | 91.0 |
| $d_1/d_2$ | 1.001 | 1.017 | 0.97 | 0.98 | 1.23 | 1.28 | 0.90 | 1.27 | 1.2 | 1.29 | 1.62 |
| $(90 - \alpha')$/° | −0.7 | −0.7 | −3.9 | −4.2 | 4.2 | 7.0 | −8.0 | 7.79 | 8.0 | 4.75 | 11.9 |
| β/° | 69.97 | 69.5 | 64.88 | 64.5 | 76.4 | 80.0 | 58 | 81.3 | 81 | 77.12 | 86.7 |
| $(\beta - 70.53)$/° | −0.56 | −1.03 | −5.6 | −6.0 | 5.9 | 9.5 | −12.5 | 10.7 | 10.5 | 6.6 | 16.2 |

* For parameter definition, see Figure 3.

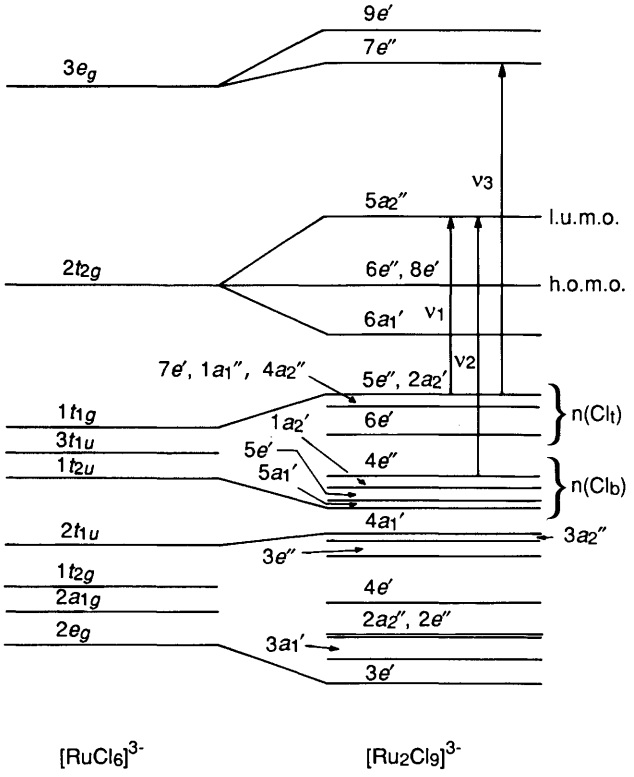


**Figure 4.** Calculated molecular orbital scheme for $[Ru_2Cl_9]^{3-}$ [28]

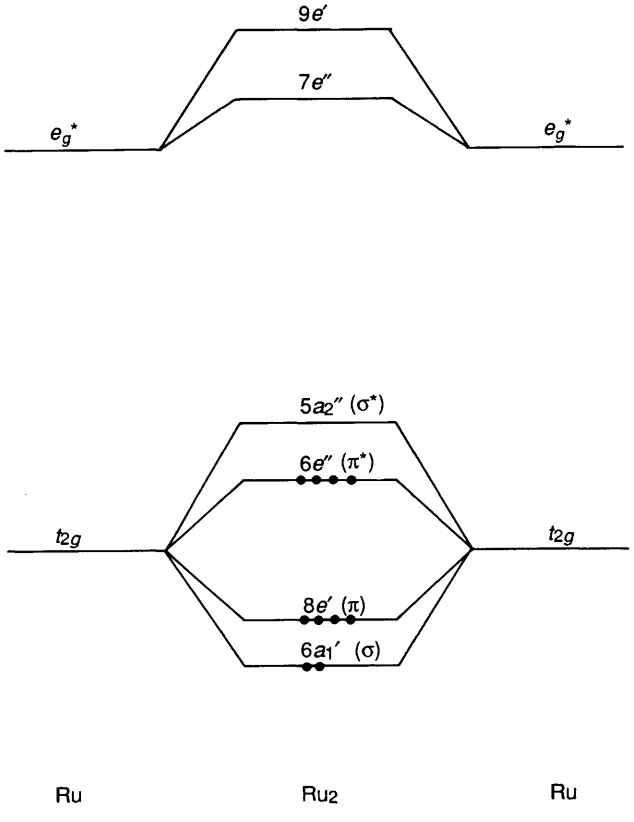


**Figure 5.** Simplified qualitative molecular orbital scheme for $[Ru_2Cl_9]^{3-}$

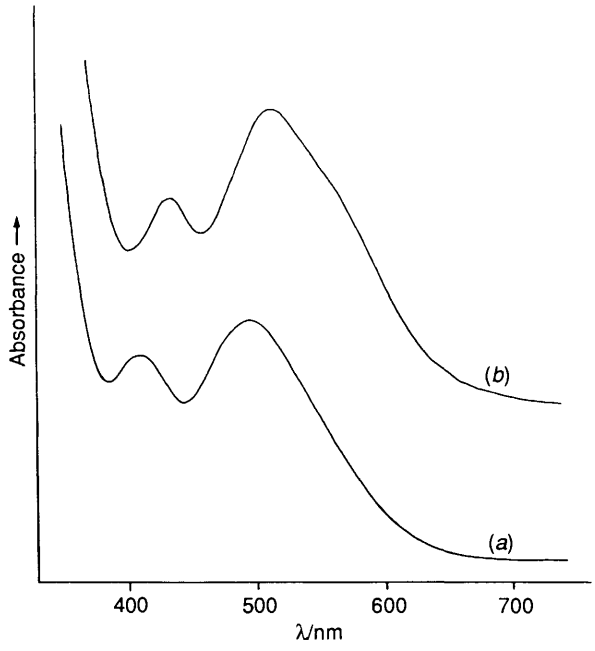


**Figure 6.** The electronic absorption spectra of $[emim]_3[Ru_2Br_9]$ in (*a*) 6 mol $dm^{-3}$ hydrobromic acid and (*b*) basic [emim]Br–$AlBr_3$ ionic liquid

known), and yet contains a significant metal–metal interaction.

*Electronic Absorption Spectroscopy of Tri-μ-bromo-bis[tribromoruthenate(III)] Salts.*—Cotton and co-workers[28] have presented the results of SCF–Xα–SW calculations upon $[Ru_2Cl_9]^{3-}$: the quantitative molecular orbital scheme for this ion is presented in Figure 4, and a simplified qualitative scheme is shown in Figure 5. Assuming that the molecular orbitals of $[Ru_2Br_9]^{3-}$ follow the same energy sequence as those calculated for $[Ru_2Cl_9]^{3-}$, then the presence of a single ruthenium–ruthenium bond in $[Ru_2Br_9]^{3-}$ can be understood in terms of the ten available *d* electrons entering the $(\sigma)^2(\pi)^4(\pi^*)^4$ orbital manifold, formed from the overlap of the $d_{xz}$, $d_{yz}$, and $d_{xy}$ orbitals.

The electronic absorption spectra of the salts $A_3[Ru_2Br_9]$ (A = Rb, Cs, or emim) in 6 mol $dm^{-3}$ hydrobromic acid and/or basic [emim]Br–$AlBr_3$ are detailed in Table 5 and illustrated in Figure 6. It is of interest that all of the bands in the spectrum recorded for the solution in the ionic liquid are moved significantly to lower energy, and exhibit a much higher $A(\nu_1)/A(\nu_2)$ ratio than do the equivalent solutions in hydrobromic acid. However, the data obtained in dichloromethane[9] more closely resemble those obtained in the ionic liquid than those obtained in hydrobromic acid. Although initially it may seem surprising that a low dielectric medium like dichloromethane should produce results similar to those found in the environment of an ionic liquid, neither solvent will support either solvation or solvolytic phenomena.[29,30] It is clear from the spectra obtained in hydrobromic acid that these solutions contain significant amounts of hydrated species, probably $[Br_3Ru(\mu\text{-}Br)_3RuBr_2(OH_2)]^{2-}$ and $[(H_2O)Br_2Ru(\mu\text{-}Br)_3RuBr_2(OH_2)]^{-}$. The spectral form suggests that the same basic chromophore is present, and indeed the visible spectra are dominated (see below) by transitions associated with the $Ru(\mu\text{-}Br)_3Ru$ moiety.

Although the near-i.r. region (4 000—15 000 $cm^{-1}$) was examined for solutions of $[emim]_3[Ru_2Br_9]$ in the basic ionic liquid, no bands were observed in this region (despite the predictions of the Xα calculations).[28] The bands $\nu_1$ (Table 5) are

**Table 5.** Electronic absorption data for $A_3[Ru_2Br_9]$

| A | Solvent | $\nu^a/cm^{-1}$ $\nu_3$[b] | $\nu_2$ | $\nu_1$ | Ref. |
|---|---|---|---|---|---|
| Rb | 6 mol $dm^{-3}$ HBr | 35 970 (29 780) | 24 750 (4 330) | 20 240 (4 620?) | *c* |
| Cs | 6 mol $dm^{-3}$ HBr | 36 100 (27 350) | 25 060 (3 730) | 20 490 (3 460?) | *c* |
| $NBu_4$ | $CH_2Cl_2$ | 34 720 (26 740) | 23 360 (4 120) | 19 720 (6 050) | 9 |
| $PPh_3(CH_2Ph)$ | $CH_2Cl_2$ | 34 970 (27 460) | 23 470 (4 970) | 19 680 (6 270) | 9 |
| emim | 6 mol $dm^{-3}$ HBr | (sh) | 24 750 (4 517) | 20 120 (5 160) | *c* |
| emim | Melt[d] | 34 720 (42 880) | 23 200 (3 400) | 19 610 (4 880) | *c* |

[a] Molar absorption coefficients ($dm^3$ $mol^{-1}$ $cm^{-1}$) in parentheses. [b] $\nu_3$ exhibits, in all cases, a low-energy shoulder at *ca.* 30 000—31 000 $cm^{-1}$. [c] This work. [d] Basic [emim]Br–$AlBr_3$ ionic liquid.

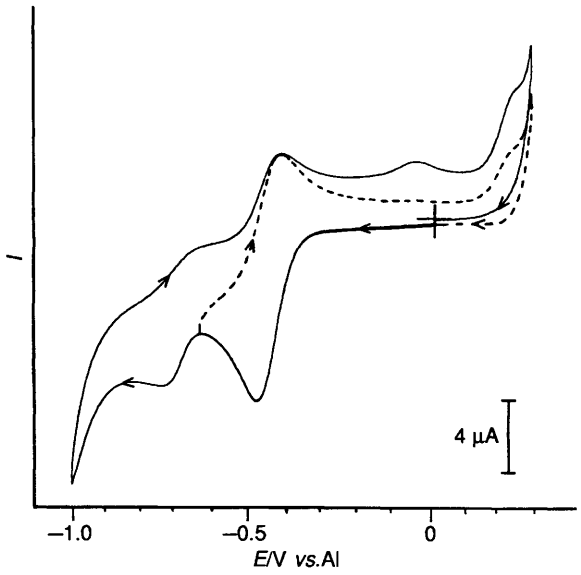


**Figure 7.** Cyclic voltammograms for a 7.13 mmol $dm^{-3}$ solution of $[Ru_2Br_9]^{3-}$ in 40.0 mol % $AlBr_3$–[emim]Br at a glassy carbon electrode: (——), scan reversed at −1.00 V; (– – –), scan reversed at −0.63 V. The scan rate was 50 mV $s^{-1}$, and the temperature was 313 K

most probably associated with ligand-to-metal charge-transfer (l.m.c.t.) transitions from the uppermost non-bonding bromine levels to the vacant Ru–Ru σ* level [*i.e.* $5e''$, $2a_2'$, $7e'$, $1a_1''$, $4a_2''$, $6e' \longrightarrow 5a_2''$; $Br_t(n) \longrightarrow RuRu(\sigma^*)$]. These uppermost non-bonding levels are principally associated with the terminal bromides, and hence $\nu_1$ is more intense in the ionic liquid and in dichloromethane than it is in hydrobromic acid (where there are less terminal bromides). The bands $\nu_2$ are similarly associated with l.m.c.t. transitions from the lower non-bonding bromine levels to the vacant Ru–Ru σ* level (*i.e.* $4e''$, $1a_2'$, $5e'$, $5a_1' \longrightarrow 5a_2''$): these lower energy non-bonding levels are associated with the bridging bromides, and so the intensity of $\nu_2$ is largely independent of solvent. Hence, the ratio $A(\nu_1)/A(\nu_2)$ is higher in $CH_2Cl_2$ and in the ionic liquid than it is in hydrobromic acid. The bands $\nu_3$ are at much higher energy, and almost certainly associated with the $5e'' \longrightarrow 7e''$ transition. These assignments, while remaining tentative, do account well for both the spectral profile and its response to a change of solvent.

*Electrochemistry of Tri-μ-bromo-bis[tribromoruthenate(III)] Salts in the* $AlBr_3$–[emim]Br *Ionic Liquid.*—A cyclic voltammogram for $[Ru_2Br_9]^{3-}$ at a glassy carbon electrode in the 40.0 mol % $AlBr_3$–[emim]Br ionic liquid is shown in Figure 7. Two reduction waves at *ca.* −0.49 and −0.75 V, respectively, can be observed for this species prior to reversing the scan at −1.00 V, and three oxidation waves at *ca.* −0.66, −0.42, and −0.05 V, respectively, can be observed when the scan is reversed following the second reduction wave. A fourth oxidation wave may also be present close to the positive limit of the solvent at *ca.* 0.22 V. However, it was not possible to examine this wave in detail, and it was not considered further. If the scan is reversed after the first reduction process, the oxidation wave at −0.05 V is not evident. In addition, if the scan rate is increased to 2 V $s^{-1}$ or greater, the second reduction wave at −0.75 V and the oxidation waves at −0.66 and −0.05 V are not present. The oxidation wave at −0.42 V is clearly associated with the reduction wave at −0.49 V, while the oxidation waves at −0.05 and −0.66 V appear to arise only after the reduction process at −0.75 V.

Detailed cyclic voltammetric data for the first reduction wave are given in Table 6. The average peak potential separation, $\Delta E_p$, for these waves, 0.073 V, is slightly larger than the theoretical value of 0.062 V expected for a one-electron, reversible c.t. reaction. In addition, the peak current ratio, $i_p^a/i_p^c$, calculated by using Nicholson's empirical method,[31] is less than 1.0:1 at the slower scan rates, but becomes essentially 1.0:1 when the scan rate is increased to 0.200 V $s^{-1}$ or greater. This behaviour is characteristic of an electron capture mechanism in which the product of the c.t. step is unstable.[32]

Taken together, these results suggest that the first reduction process at −0.49 V corresponds to the reduction of $[Ru_2Br_9]^{3-}$ to $[Ru_2Br_9]^{4-}$, which is unstable at slow scan rates and decomposes to a product that can be reduced at −0.75 V. A first-order homogeneous rate constant of 0.07 $s^{-1}$ at 313 K was estimated for the decomposition of $[Ru_2Br_9]^{4-}$ by using double-potential-step chronoamperometry.[33] The oxidation of $[Ru_2Br_9]^{4-}$, produced by the reduction of $[Ru_2Br_9]^{3-}$, can also be observed in $CH_2Cl_2$ by using cyclic voltammetry, but the experiment must be conducted at 233 K.[9] Thus, the latter species appears to be considerably more stable in the $AlBr_3$–[emim]Br ionic liquid than in $CH_2Cl_2$.

A diffusion coefficient of $8.6 \times 10^{-8}$ $cm^2$ $s^{-1}$ was calculated for $[Ru_2Br_9]^{3-}$ from the average value of $i_p^c/\nu^{\frac{1}{2}}$ given in Table 6. Consideration of the viscosity of the ionic liquid at 313 K, 0.395 g $cm^{-1}$ $s^{-1}$,[8] yields a Stokes–Einstein product of $3.4 \times 10^{-8}$ g cm $s^{-2}$. This value is somewhat different from the Stokes–Einstein product that was calculated from the diffusion coefficient of $[Ru_2Br_9]^{3-}$ in $CH_2Cl_2$ at 285 K, $2.2 \times 10^{-8}$ g cm $s^{-2}$.[9]

*Upon the Non-existence of μ-Oxo-bis[pentabromoruthenate(IV)] Salts.*—Many attempts were made to prepare the salts $A_4[Ru_2OBr_{10}]$ (A = Cs or Rb) by the method of San Filippo *et al.*[4,5] by variations upon that method, and by alternative methods that had previously been used to prepare $A_4[Ru_2OCl_{10}]$ (see Experimental section). None of these methods was successful: the only ruthenium-containing products isolated

**Table 6.** Voltammetric data for $[emim]_3[Ru_2Br_9]$ in 40.0 mol % $AlBr_3$ – [emim]Br

| $\nu$/V s$^{-1}$ | $-E_p^c$/V | $-E_{\frac{1}{2}}^*$/V | $\Delta E_p$/V | $10^5 i_p^c \nu^{-\frac{1}{2}}$/A s$^{\frac{1}{2}}$ V$^{-\frac{1}{2}}$ | $i_p^a/i_p^c$ |
|---|---|---|---|---|---|
| 0.010 | 0.492 | — | — | 4.2 | 0.67 |
| 0.020 | 0.495 | 0.458 | 0.075 | 4.1 | 0.72 |
| 0.050 | 0.496 | 0.460 | 0.073 | 4.0 | 0.82 |
| 0.100 | 0.497 | 0.461 | 0.072 | 4.0 | 0.92 |
| 0.200 | 0.500 | 0.463 | 0.074 | 3.9 | 1.02 |
| 0.500 | 0.485 | 0.453 | 0.075 | 3.9 | 1.06 |
| 1.000 | 0.482 | 0.449 | 0.067 | 3.9 | 1.06 |

* Estimated from $(E_p^a + E_p^c)/2$.

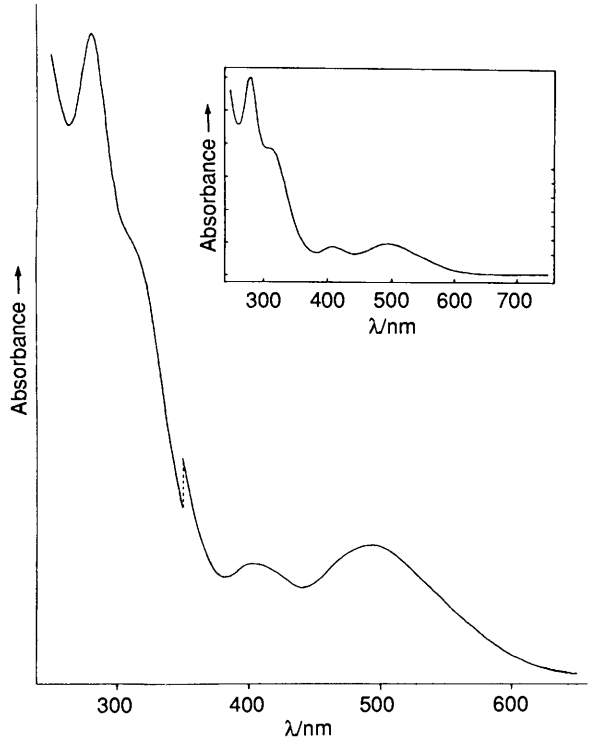


**Figure 8.** The electronic absorption spectrum of $Cs_3[Ru_2Br_9]$ in 6 mol dm$^{-3}$ hydrobromic acid, compared with that obtained by San Filippo *et al.*[4,5] for '$Cs_4[Ru_2OBr_{10}]$' in 5 mol dm$^{-3}$ hydrobromic acid (see inset)

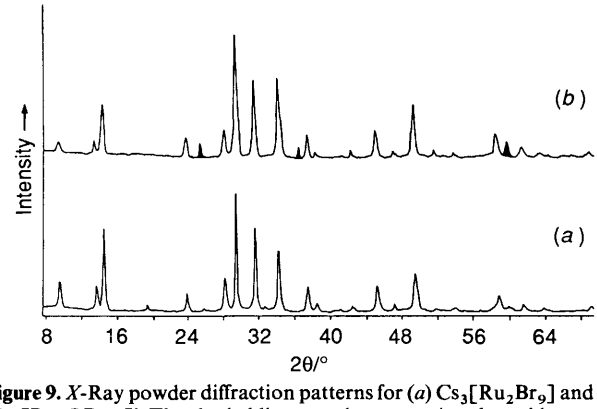


**Figure 9.** *X*-Ray powder diffraction patterns for (*a*) $Cs_3[Ru_2Br_9]$ and (*b*) '$Cs_4[Ru_2OBr_{10}]$'. The shaded lines are due to caesium bromide

were $A_3[Ru_2Br_9]$ and $A_2[RuBr_6]$, as indicated by electronic absorption spectroscopy, *X*-ray powder diffraction, and i.r. spectroscopy. Indeed, the ready interconversion of $A_3[Ru_2Br_9]$ and $A_2[RuBr_6]$ has been noted elsewhere.[7,16] The rubidium and caesium salts prepared by the exact method of San Filippo *et al.*[4,5] gave electronic spectra in hydrobromic acid identical to the one reported by those workers (see Figure 8) and identical to the spectra of $A_3[Ru_2Br_9]$ reported here. Moreover, the powder *X*-ray diffraction patterns obtained for '$A_4[Ru_2OBr_{10}]$' (A = Cs or Rb) correspond to a mixture of $A_3[Ru_2Br_9]$ and ABr (see Figure 9), and their i.r. spectra are indistinguishable from those of pure $A_3[Ru_2Br_9]$. The resonance-Raman data of San Filippo *et al.*[4,5] for '$A_4[Ru_2OBr_{10}]$' (A = Cs or Rb) can thus be understood in terms of the excitation at 20 300 cm$^{-1}$ {$\nu_1$; $Br_t(n) \longrightarrow RuRu(\sigma^*)$ for $[Ru_2Br_9]^{3-}$} stimulating a Raman band at 247 cm$^{-1}$ [$\nu$(RuBr)$_t$, see above], and their analytical data can be interpreted in terms of a 1:1 mixture of $A_3[Ru_2Br_9]$ and ABr.

In summary, we can find no evidence that μ-oxo-bis-[pentabromoruthenate(IV)] salts exist or have ever been prepared. That does not, of course, mean that they cannot be prepared, merely that routes analogous to those used for the chloride complexes are unsuccessful.

## Appendix

*Analysis of the* X-*Ray Diffraction Powder Patterns.*—For a hexagonal system, the line positions are defined by equation (A1), where $A = \lambda^2/3a_0^2$ and $C = \lambda^2/4c_0^2$.[15] For the $\langle hk0 \rangle$ lines, equation (A1) reduces to (A2), and for the $\langle 00l \rangle$, equation

$$\sin^2\theta = A(h^2 + hk + k^2) + Cl^2 \quad \text{(A1)}$$

$$\sin^2\theta = A(h^2 + hk + k^2) \quad \text{(A2)}$$

(A1) reduces to (A3). Hence, by treating the $\langle hk0 \rangle$ and $\langle 00l \rangle$ lines separately, $a_0$ and $c_0$ were calculated and found to be a regular function of θ. In order to determine the ideal lattice parameters (*i.e.* for $2\theta = 180°$), the values of $a_0(\theta)$ and $c_0(\theta)$ were plotted against the Nelson–Riley function, *N*, which is defined in equation (A4).[15] Using a conventional linear

$$\sin^2\theta = Cl^2 \quad \text{(A3)}$$

$$N = (\cos^2\theta/\sin^2\theta) + [(\cos^2\theta)/\theta] \quad \text{(A4)}$$

regression procedure, and rejecting all values for $2\theta < 30°$, a straight line was fitted to the data and extrapolated to $N = 0$ (*i.e.* $2\theta = 180°$). These values of the two lattice parameters were scaled by the calibration factor to yield the values reported in Table 2.

## Acknowledgements

We thank the S.E.R.C. for a postdoctoral fellowship (to J. E. T.), the Venture Research Unit (BP) for financial support, and Basrah University, Iraq, for a scholarship (to J. A. Z.). Work performed at the University of Mississippi was supported by National Science Foundation grants nos. CHE-8412730 and CHE-8715464, and funds for collaborative research were provided by N.A.T.O. grant no. 020/84.

## References

1 E. A. Seddon and K. R. Seddon, 'The Chemistry of Ruthenium,' Elsevier, Amsterdam, 1984, (*a*) pp. 97—101, 153; (*b*) pp. 159—160; (*c*) p. 161.
2 J-P. Deloume, R. Faure, and G. Thomas-David, *Acta Crystallogr., Sect. B*, 1979, **35**, 558.
3 A. McL. Mathieson, D. P. Mellor, and N. C. Stephenson, *Acta Crystallogr.*, 1952, **5**, 185.
4 J. San Filippo, jun., P. J. Fagan, and F. J. Di Salvo, *Inorg. Chem.*, 1977, **16**, 1066.
5 J. San Filippo, jun., R. L. Grayson, and H. J. Sniadoch, *Inorg. Chem.*, 1976, **15**, 269.

6 D. Appleby, R. I. Crisp, P. B. Hitchcock, C. L. Hussey, T. A. Ryan, J. R. Sanders, K. R. Seddon, J. E. Turp, and J. A. Zora, *J. Chem. Soc., Chem. Commun.*, 1986, 483.
7 J. E. Fergusson and A. M. Greenaway, *Aust. J. Chem.*, 1978, **31**, 497.
8 J. R. Sanders, E. H. Ward, and C. L. Hussey, *J. Electrochem. Soc.*, 1986, **133**, 325, 1526.
9 V. T. Coombe, G. A. Heath, T. A. Stephenson, and D. K. Vattis, *J. Chem. Soc., Dalton Trans.*, 1983, 2307.
10 T. B. Scheffler and C. L. Hussey, *Inorg. Chem.*, 1983, **22**, 1279.
11 C. L. Hussey and H. A. Øye, *J. Electrochem. Soc.*, 1984, **131**, 1621.
12 R. I. Crisp, D.Phil. Thesis, University of Oxford, 1982.
13 P. Main, MULTAN, A system of computer programs for automatic solution of crystal structure from *X*-ray diffraction data, York University, July 1982.
14 'International Tables for *X*-Ray Crystallography,' Kynoch Press, Birmingham, 1974, vol. 4.
15 B. D. Culity, 'Elements of *X*-Ray Diffraction,' Addison-Wesley, Reading, Massachusetts, 1978.
16 C. L. Hussey, J. R. Sanders, T. A. Ryan, D. Appleby, P. B. Hitchcock, K. R. Seddon, J. E. Turp, and J. A. Zora, *J. Chem. Soc., Dalton Trans.*, to be submitted.
17 J. R. Ferraro, 'Low Frequency Vibrations of Inorganic and Coordination Compounds,' Plenum, New York, 1971.
18 A. K. Abdul-Sada, A. M. Greenway, P. B. Hitchcock, T. J. Mohammed, K. R. Seddon, and J. A. Zora, *J. Chem. Soc., Chem. Commun.*, 1986, 1753.
19 P. B. Hitchcock, T. J. Mohammed, K. R. Seddon, J. A. Zora, C. L. Hussey, and E. H. Ward, *Inorg. Chim. Acta*, 1986, **113**, L25.
20 J. Darriet, *Rev. Chim. Miner.*, 1981, **18**, 27.
21 R. Saillant, R. B. Jackson, W. E. Streib, K. Floting, and R. A. D. Wentworth, *Inorg. Chem.*, 1971, **10**, 1453.
22 G. J. Wessel and D. J. W. Ijdo, *Acta Crystallogr.*, 1957, **10**, 466.
23 W. H. Watson, jun., and J. Waser, *Acta Crystallogr.*, 1958, **11**, 689.
24 F. A. Cotton and D. A. Ucko, *Inorg. Chim. Acta*, 1972, **6**, 161.
25 H. M. Powell and F. A. Wells, *J. Chem. Soc.*, 1935, 1008.
26 O. Lindquist, *Acta Chem. Scand.*, 1968, **22**, 2943.
27 T. J. Kistenmacher and G. D. Stucky, *Inorg. Chem.*, 1971, **10**, 122.
28 B. E. Bursten, F. A. Cotton, and A. Fang, *Inorg. Chem.*, 1983, **22**, 2127.
29 D. Appleby, C. L. Hussey, K. R. Seddon, and J. E. Turp, *Nature (London)*, 1986, **323**, 614.
30 K. R. Seddon, in 'Molten Salt Chemistry: An Introduction and Selected Applications,' eds. G. Mamantov and R. Marassi, NATO ASI Series C, 1987, vol. 202, 365.
31 R. S. Nicholson, *Anal. Chem.*, 1966, **38**, 1406.
32 R. S. Nicholson and I. Shain, *Anal. Chem.*, 1964, **36**, 706.
33 W. M. Schwarz and I. Shain, *J. Phys. Chem.*, 1965, **69**, 30.

*Received* 19*th October* 1989; *Paper* 9/04498A